Synthesis dynamics of passivated silicon nanoclusters

ARTICLE *in* PHYSICA STATUS SOLIDI (B) · SEPTEMBER 2003

Impact Factor: 1.49 · DOI: 10.1002/pssb.200303232

4 AUTHORS:

Erik Draeger
Lawrence Livermore National Laboratory
29 PUBLICATIONS **677** CITATIONS
SEE PROFILE

Jeffrey Grossman
Massachusetts General Hospital
228 PUBLICATIONS **5,886** CITATIONS
SEE PROFILE

Andrew Williamson
True North Venture Partners
106 PUBLICATIONS **3,805** CITATIONS
SEE PROFILE

Giulia Galli
University of California, Davis
452 PUBLICATIONS **12,519** CITATIONS
SEE PROFILE

phys. stat. sol. (b) **239**, No. 1, 11–18 (2003) / **DOI** 10.1002/pssb.200303232

Synthesis dynamics of passivated silicon nanoclusters

Erik W. Draeger*, **Jeffrey C. Grossman, Andrew J. Williamson,** and **Giulia Galli**

Lawrence Livermore National Laboratory, P.O. Box 808, Livermore, CA 94550, USA

Received 15 March 2003, revised 15 May 2003, accepted 15 June 2003
Published online 1 September 2003

PACS 61.46.+w, 78.67.Bf

The effect of preparation conditions on the structural and optical properties of silicon nanoparticles is investigated using first-principles molecular dynamics and quantum Monte Carlo techniques. We find that high-temperature synthesis processes can produce kinetically-limited nanostructures with different core structures than bulk-derived crystalline clusters. These nanoparticles have optical gaps in better agreement with experimental measurements than crystalline clusters of the same size. The type of core structure that forms from a given synthesis process may depend on the passivation mechanism and time scale.

In recent years, there has been a considerable amount of theoretical and experimental interest focused on silicon nanoclusters [1–4]. A combination of the unique optical properties of silicon quantum dots and their compatability with existing silicon-based and nano-biological technologies demonstrates great promise for numerous applications. For clusters between 1–3 nm in diameter, the size range in which Si quantum dots may exhibit luminescence in the visible wavelengths, a range of optical properties have been measured for clusters synthesized using different techniques [4–9]. For example, the optical gaps of silicon clusters formed by physical vapor deposition [10] were found to be several eV lower than those formed using inverse micelles [11]. Even quantum dots made via the same process have been found to exhibit widely-varying absorption and emission spectra, perhaps due to small differences in preparation conditions and limitations in the accuracy of characterization techniques. These discrepancies pose a significant challenge to the practical application of silicon quantum dots and demonstrate the need for accurate theoretical predictions to help guide experiments.

One of the fundamental challenges to theoretical investigation of nanoclusters is the choice of atomic configurations. Previous theoretical studies of silicon nanoclusters have used either crystalline [12] or quasi-amorphous structural templates [13] to generate the coordinates of the nanocluster, which is assumed to be a spherical piece of bulk material, with any dangling bonds at the surface fully passivated with hydrogen. For crystalline clusters larger than 3 nm, calculated optical gaps have been shown to be in good agreement with experiment [14]. For smaller clusters, where a significant fraction of the atoms compose a more highly curved surface, it is not clear that the use of bulk-derived structures is appropriate.

In this paper, we investigate the types of metastable low-strain structures that are likely to be produced from a given synthesis process. In order to take into account the subtle dynamical effects needed for accurate predictions, we used first-principles molecular dynamics (FPMD) and quantum Monte Carlo (QMC) calculations to determine the impact of the experimental synthesis process on the structural and optical properties of 1 nm silicon dots. Our results indicate that when a finite-tempera-

* Corresponding author: e-mail: draeger1@llnl.gov, Phone: (925)423-3650, Fax: (925)422-6594

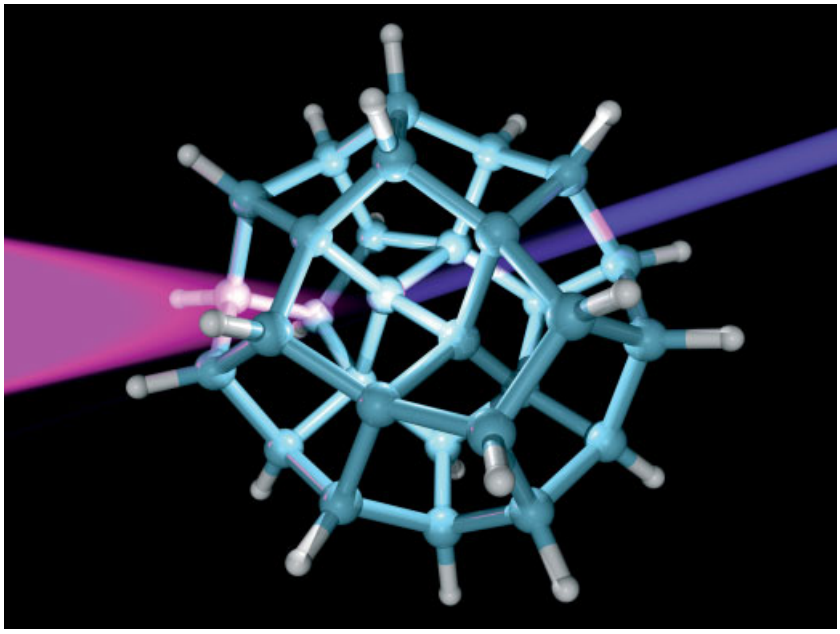

Fig. 1 Prototype silicon quantum dot formed by high-temperature synthesis. According to our calculations, this 1 nm structure luminesces at $\sim$400 nm (ultraviolet).

ture synthesis and passivation process is emulated, the number of atoms in the core of the resulting cluster is larger than for ideal, bulk-derived structures. For 1 nm silicon nanoclusters, this results in clusters with a double tetrahedral core consistently emerging, rather than bulk-derived single-core structures. We find that double-core structures with 30 silicon atoms are favored by symmetry, instead of the 29 silicon atoms favored in a single-core crystalline cluster. The optical gaps of double-core clusters produced by FPMD simulations are consistently in good agreement with experiment (see Fig. 1). In contrast, the optical gaps of crystalline single-core structures are significantly larger than current experimental measurements.

We observe a subtle interplay between the strain associated with high curvature and surface dangling bonds and the preference for silicon to form tetrahedrally-symmetric cores. We show that these two competing effects produce a class of structures defined by the core geometry and the bonding of the core atoms to the surface. Rather than a search for low-energy structures, this classification results from a careful examination of the metastable, kinetically-limited nanostructures produced by FPMD, and can be applied to other nanoscale systems. We also show that structures which are likely to form via a given synthesis method strongly depend on the mechanism by which the silicon surface is passivated and on the ability to satisfy surface strain during the growth sequence.

In order to accurately account for bond breaking and formation processes during passivation, the Car-Parinello FPMD approach was employed, such that electronic degrees of freedom are solved quantum mechanically while the ions move classically. Our FPMD and density functional theory calculations were carried out using a first-principles molecular dynamics code, GP 1.16.0 [15]. The local density approximation (LDA) was used, with the Ceperley–Alder exchange-correlation functional [16]. A time step of 0.075 fs was used in the molecular dynamics simulations. Clusters were placed in a periodic box with at least 7 Å of vacuum region between periodic replicas. We used norm conserving non-local pseudopotentials of the Hamann type [17] for the silicon atoms, and the Giannozzi type [18] for the hydrogen atoms. The Kohn–Sham orbitals were expanded in plane waves with a kinetic energy cutoff of 35 Ry.

Several experimental techniques for synthesizing silicon nanoparticles, such as physical vapor deposition [10] and laser ablation [19], generate a high temperature silicon vapor from which nanoclus-

ters nucleate as the vapor cools. During or after cooling, there is typically exposure to some form of passivant (e.g., hydrogen, oxygen) which removes dangling bond states from the surface of the cluster. To simulate this process, we start from an amorphous cluster obtained by heating a bare silicon cluster (with ideal crystalline geometry) at 1500 K for $\sim$3 ps to remove any "memory" of the initial conditions. A new hydrogen atom is added to the surface every 0.45–0.75 ps until all silicon atoms are four-fold coordinated. Several different algorithms for attaching the hydrogens to available surface silicon atoms were tested. Most of the simulations performed used an algorithm in which a new hydrogen atom is placed on the available (i.e. a silicon atom with less than four neighbors) surface silicon which is farthest from any other hydrogen, so as to maximize the overall uniformity of hydrogen on the surface. Other rules we employed to choose between multiple available passivation sites included choosing surface silicon atoms with the maximum number of dangling bonds, maximizing the new hydrogen distance from the cluster center of mass and/or simple random sampling. We found that as long as hydrogen atoms were attached to silicon atoms that had a coordination number of less than four, the results were independent of the algorithm (and hence the order) by which hydrogen atoms were attached to the surface. Simple thermodynamic arguments, assuming atmospheric pressure and ideal gas vapor densities, predict an additional hydrogen will passivate the surface every 1–2 ps. By using a series of elevated temperatures ($T = 600$, 800, and 1000 K), we were able to observe realistic passivation events on shorter time scales (0.45–0.75 ps) while confirming that the higher temperatures did not qualitatively alter the growth process. For each system, multiple simulations were

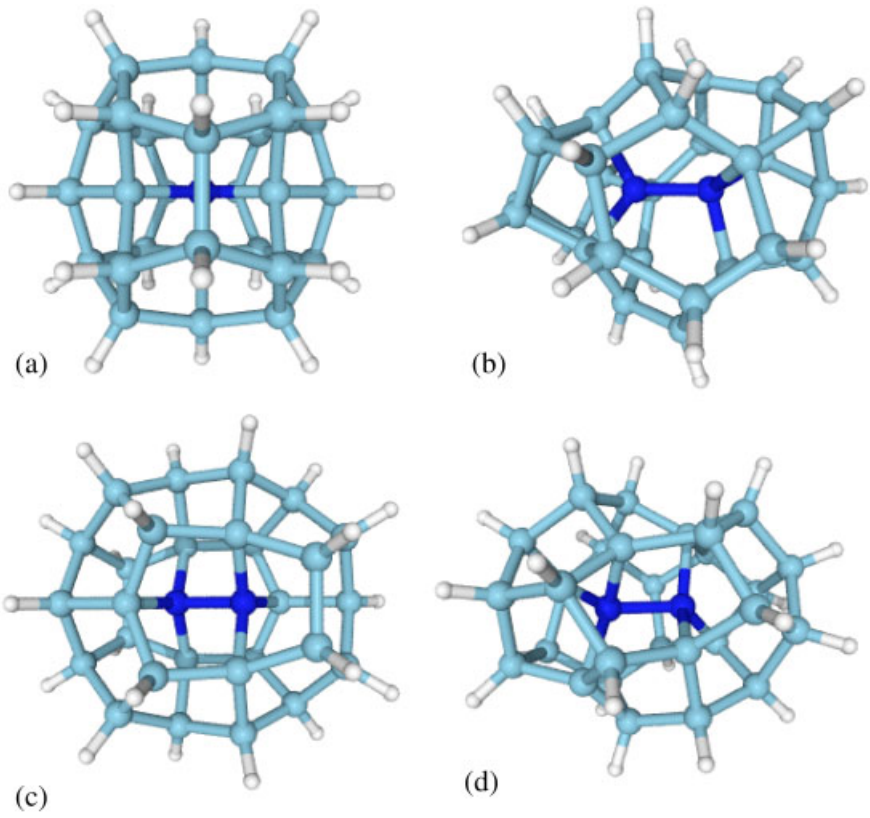

Fig. 2 Results of FPMD synthesis for Si_{29} and Si_{30}, compared with low-energy ideal structures. Interior core atoms are dark blue. a) Ideal $Si_{29}H_{24}$ structure proposed in Ref. [12]; b) representative final $Si_{29}H_{21}$ structure from FPMD synthesis at $T = 1000$ K, relaxed at $T = 0$ K; c) proposed ideal $Si_{30}H_{22}$ structure; d) representative final $Si_{30}H_{22}$ structure from FPMD synthesis at $T = 1000$ K, relaxed at $T = 0$ K.

carried out from different starting points in order to obtain a statistically representative sample. The combined total simulation time for all clusters investigated here was $\sim$750 ps.

The present work focuses on the 1 nm size range where there are $\sim$30 silicon atoms per quantum dot. We performed simulations starting from amorphous Si_{29}, Si_{30}, and Si_{31}. Surprisingly, in our simulations which started from Si_{29}, the single tetrahedral core structure predicted for 29 silicon atoms (see Fig. 2a) does not form. Instead, we found that the resulting passivated structures consistently had a *double* tetrahedral core – two interior silicon atoms rather than one (see Fig. 2b). The formation of a double core was found to be completely independent of temperature and the order in which hydrogen atoms were added to the surface. Eight separate synthesis calculations starting from amorphous Si_{29} all resulted in double-core structures. The resulting Si_{29} structures were highly strained due to the lack of a symmetric arrangement of 21 surface silicon atoms around the 8-atom double core structure.

The explanation for the consistent formation of a double-core structure lies with the dynamics of bare silicon clusters. Above $T = 300$ K, unpassivated crystalline nanoclusters become amorphous, with multiple atoms in the center of the cluster attempting to saturate the dangling bonds of the surface atoms. 1 nm clusters of amorphous silicon typically have two to three such highly coordinated interior atoms. As hydrogens are added to the surface, the number of dangling bonds is reduced and the interior atoms develop stable bonds to the surface. As long as a majority of the atoms at the surface are unpassivated, it is energetically favorable for two interior atoms to each passivate three dangling bonds, to form an eight atom double tetrahedral core. Passivation has the effect of "freezing" that region of the cluster surface as atoms at the surface become four-fold coordinated. By the time enough hydrogens have been added to fully passivate the surface, the cluster surface has frozen around a double-core structure. During formation, there is no clear pathway to a single-core structure in this type of synthesis process, as forming a single-core cluster from bare silicon requires a portion of the surface to sustain multiple dangling bonds until enough hydrogen atoms have been added to fully passivate the surface, a situation likely to occur only when starting from a bare crystalline cluster at low temperature or with rapid passivation. Once a double-core cluster is formed, a transition to a single-core structure involves a global reconstruction of the surface, with multiple events involving the simultaneous breaking of several silicon bonds, and thus is expected to have a large barrier.

By symmetry, 30 silicon atoms are more favorable than 29 atoms for the formation of 1 nm double-core nanoclusters. Six subsequent simulations of hydrogen passivation of amorphous Si_{30} at $T = 600$ K and $T = 1000$ K, using the same FPMD synthesis calculations as for Si_{29}, again consistently produced double-core structures. The simulation dynamics of Si_{29} and Si_{30} were qualitatively very similar. However, for Si_{30} FPMD produced many low-energy structures (the example shown in Fig. 2d had a total energy which is only 0.1 eV higher than the proposed ideal structure Fig. 2c) that are qualitatively similar to the ideal high-symmetry structure. $Si_{30}H_{22}$ has a symmetric ideal construction which can be represented as a 28-atom cage (14 pentagons, 2 septagons) surrounding two interior atoms (Fig. 2c). To test stability, we heated this structure at $T = 1000$ K for 10 ps, and found it to be stable to thermodynamic fluctuations. Similar to Si_{29}, Si_{31} also produced double-core structures, again significantly more strained than those starting from Si_{30}.

To study how the core structure evolves as the synthesis simulation progresses, we need a quantitative measure of whether a given silicon atom is in the interior of the cluster. We define the degree to which an atom is in the interior by the fraction of the total solid angle around atom i that is not occupied by other silicon atoms. For simplicity, we approximate this solid angle by calculating the maximum base angle Ω of a cone whose apex is centered on atom i and whose volume does not intersect any other silicon atoms (see Fig. 3 inset):

$$\Omega_i = \max\{\theta_1, \cdots, \theta_{i-1}, \theta_{i+1}, \cdots, \theta_N\} - \min\{\theta_1, \cdots, \theta_{i-1}, \theta_{i+1}, \cdots, \theta_N\} \quad (1)$$

where $0 \leq \theta_j < 2\pi$ is the angle atom j makes with the axis defined by the vector from the center of mass to atom i, translated so that atom i is at the origin (the center of mass is at $\theta = \pi$). An atom in the center of an infinite solid will have a value of Ω which approaches zero. For a small nanocluster, the minimum value of Ω for an interior atom is roughly 30 degrees, due to the finite number of atoms. An atom at the surface will typically have a value of $120 < \Omega < 230$ degrees, depending on

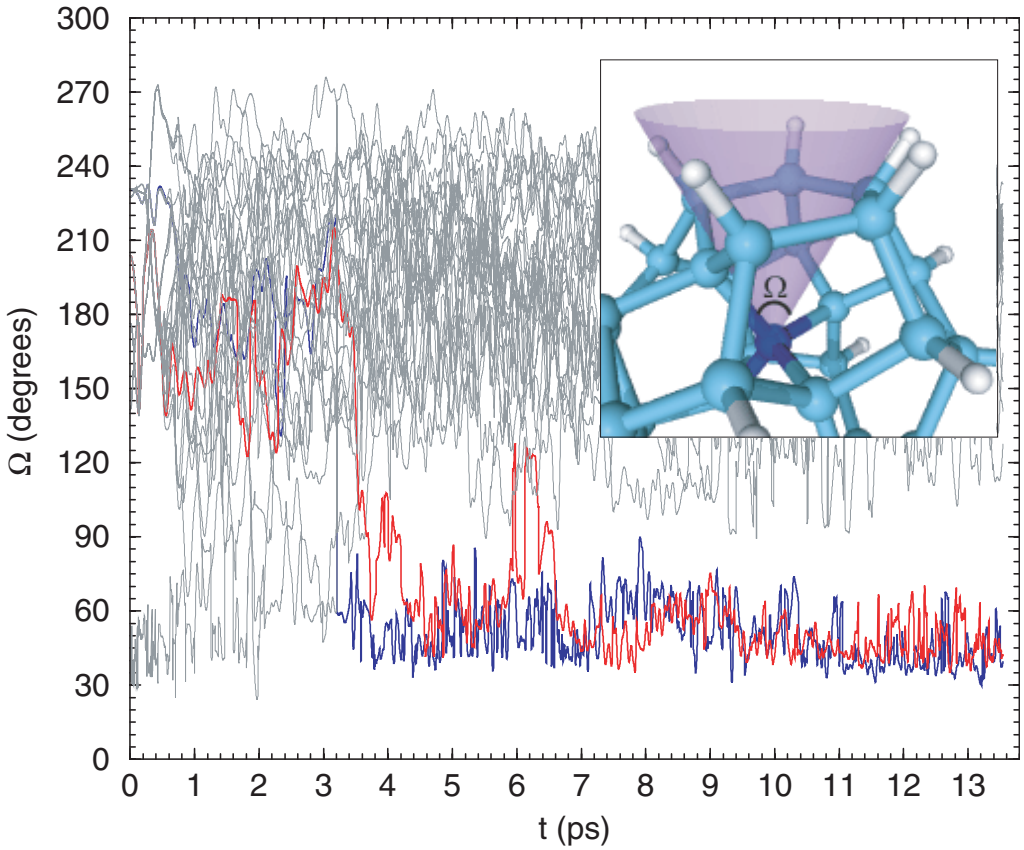

Fig. 3 Maximum solid angle unoccupied by other silicon atoms Ω_i (see text) vs. time in an Si_{29} FPMD synthesis run. The bare cluster is heated at $T = 1500$ K for 3 ps, then run at $T = 1000$ K, with a hydrogen atom added to the surface of the cluster every 0.45 ps. The blue and red curves correspond to the two interior core atoms, and the grey curves are surface silicon atoms by the end of the simulation. The inset shows how Ω is defined, in this case for an interior atom (dark blue).

whether it is part of core (and hence directly bonded to an interior atom) or a surface atom passivated with hydrogen.

The quantity Ω is plotted as a function of time in Fig. 3 for a simulation of the synthesis of Si_{29}, starting from an unpassivated crystalline cluster. Within 0.75 ps of the initial 3 ps heating at 1500 K, an atom has moved from the surface to become a second core atom in the cluster. In the early stages of the synthesis process, before many hydrogen atoms have been added to the surface, fluctations in Ω are large, and exchange of interior and surface atoms is common. Once roughly half of the surface dangling bonds are passivated, the fluctuations in Ω of the interior atoms decrease considerably.

A number of different experimental synthesis processes have been used to make silicon quantum dots. Recently, silicon nanoclusters with discrete cluster sizes have been produced by etching and sonification of porous silicon [20]. In this process, silicon clusters are formed by breaking apart larger pieces of hydrogenated silicon – a fundamentally different synthesis process to the silicon vapor based techniques described above, since the starting point is crystalline bulk, not amorphous vapor. During these room-temperature experiments, the sonficiation process will produce partially-passivated nanocrystalline fragments; however, it is not clear whether these fragments will retain a crystalline core, or whether double-core structures will form. In order to estimate the stability of the crystalline

core in these cases, we focus on determining the number of hydrogens required to maintain a single-core crystalline structure at high temperature.

To this end, we performed FPMD simulations in which a number of neighboring hydrogen atoms were removed from a tetrahedrally symmetric $Si_{29}H_{24}$ nanocrystal, which was then heated to $T = 600$ K and 1000 K. At $T = 1000$ K, removal of only 6 hydrogen atoms ($Si_{29}H_{18}$, see Fig. 1a) resulted in a persistantly stable, single-core structure. When 12 hydrogen atoms were removed ($Si_{29}H_{12}$), the silicon cluster formed a double core within 0.75 ps. When 18 hydrogen atoms were removed ($Si_{29}H_6$), the cluster formed a double core within 0.75 ps, but also exhibited dynamics consistent with an amorphous cluster, as shown by the exchange of interior core and surface atoms on a time scale of roughly 1.5 ps (Fig. 1d). We found that 14 neighboring hydrogen atoms ($Si_{29}H_{14}$) are required to maintain a single tetrahedral core. At $T = 600$ K, similar behavior is observed, although the double-core formed more slowly than at $T = 1000$ K. Based on these findings, it is possible that a 1 nm nanocluster exhibiting bulk-like crystallinity can be formed from the break-up of larger passivated clusters, as long as more than half the surface of the resulting nanocluster is passivated within picoseconds of break up.

Even if the 1 nm nanoclusters formed with porous sonification are in fact crystalline, the measured optical gaps are not in agreement with the lowest-energy crystalline $Si_{29}H_{24}$ structure. A bulk-like surface reconstruction of crystalline $Si_{29}H_{36}$ to $Si_{29}H_{24}$ was proposed [12] (see Fig. 2a) and found to have an optical gap in agreement with an experimentally-measured optical gap of 3.44 eV for 1 nm clusters synthesized using porous sonification [20]. We find two reconstructions of $Si_{29}H_{24}$ which are ~ 1 eV lower in energy, with optical gaps significantly larger than 3.5 eV. These reconstructions are unique to a curved nanosurface, and are discussed in more detail in a separate study [21].

To calculate optical gaps that are directly comparable with experiment, we employ the highly accurate fixed-node diffusion Monte Carlo method. In our DMC approach [22, 23], version 1.5.4 of the CASINO code [24], we use an optimized correlated, many-body trial wave function which is a product of Slater determinants and a correlation factor; we use non-local pseudopotentials to treat atomic cores, and fixed geometries taken from FPMD calculations. Our calculated QMC optical gap for ideal $Si_{30}H_{22}$ is 3.2(1) eV, while the lowest-energy $Si_{29}H_{24}^{nano2}$ structure has an optical gap of 4.1(1) eV. As mentioned, there exist two other $Si_{29}H_{24}$ structures, with optical gaps of 3.5(1) eV and 4.5(1) eV. In Table 1, a range of LDA gaps for $Si_{29}H_{22}$ and $Si_{30}H_{22}$ clusters generated by high temperature FPMD synthesis is provided to give an estimate of statistical variation of the results.

The QMC optical gap given in Table 1 was calculated using the final coordinates of the FPMD synthesis simulation which had the largest LDA gap. The QMC gaps can be directly compared with experimental absorption data, and shows that the clusters produced by high temperature FPMD synthesis are in good alignment with experiment [9, 20]. It should be emphasized that this is not intended to imply that these experiments must be producing non-crystalline clusters, but simply that non-crystalline clusters can form with optical gaps comparable with the largest that have been observed experimentally. For $Si_{29}H_{22}$, the optical gaps of the double-core structures produced by FPMD synthesis are significantly smaller than those of the high-symmetry crystalline $Si_{29}H_{24}$ single-core clusters, but are in good agreement with those of the FPMD $Si_{30}H_{22}$ structures and the proposed ideal $Si_{30}H_{22}$ sym-

Table 1 Energy gaps for silicon nanoclusters, calculated using both LDA and QMC. For structures created with FPMD, a range of LDA gap energies is given, with QMC gaps calculated only for the structure with the largest LDA gap.

	E_{gap}^{LDA} (eV)	E_{gap}^{QMC} (eV)
$Si_{29}H_{22}^{FPMD}$	2.2–2.3	3.3(1)
$Si_{29}H_{24}^{nano2}$	2.9	4.1(1)
$Si_{30}H_{22}^{ideal}$	2.2	3.2(1)
$Si_{30}H_{22}^{FPMD}$	2.2–2.4	3.4(1)

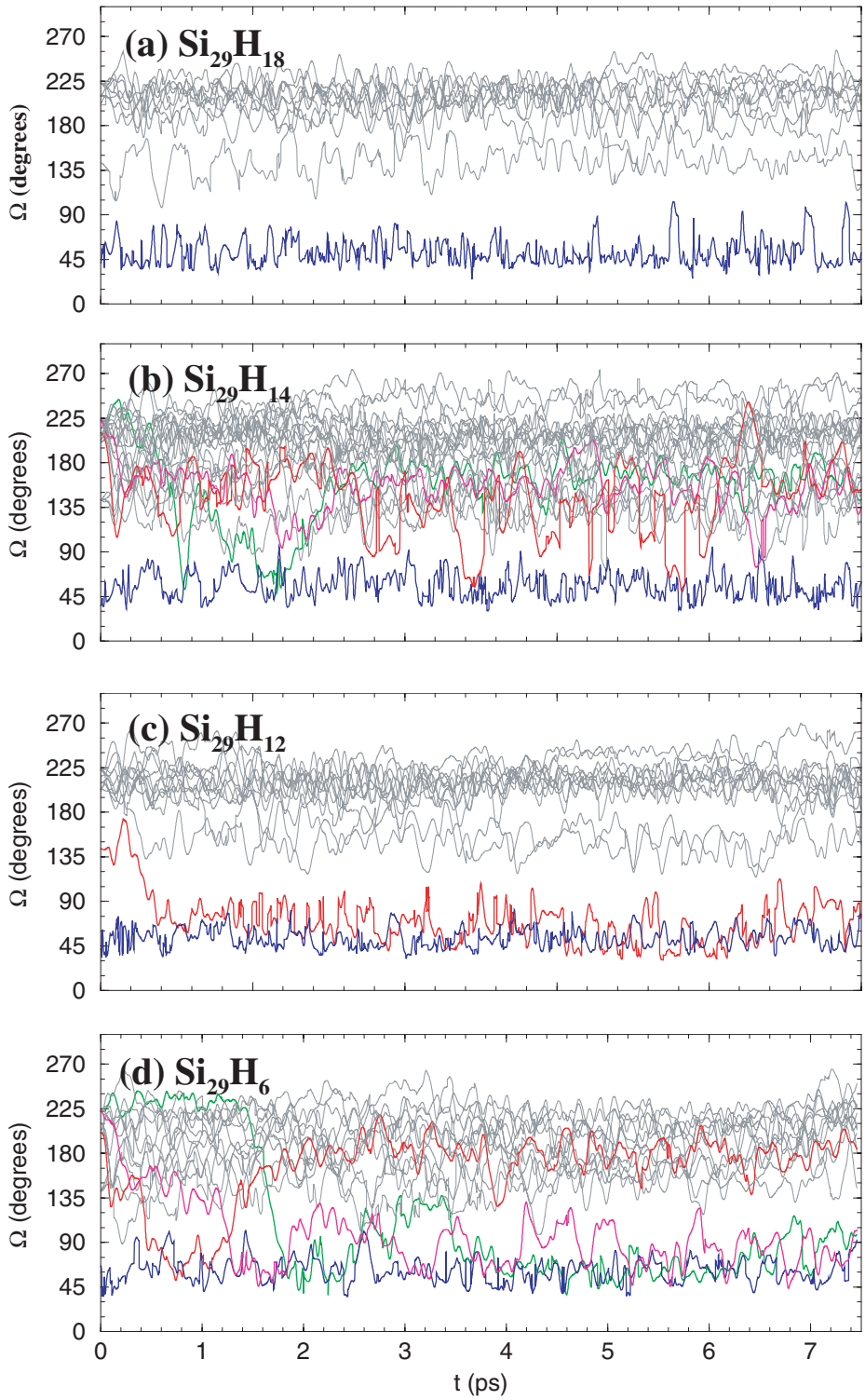

Fig. 4 Interior parameter Ω_i vs. time for the silicon atoms in a) $Si_{29}H_{18}$, b) $Si_{29}H_{14}$, c) $Si_{29}H_{12}$, and d) $Si_{29}H_6$ FPMD simulations at $T = 1000$ K. The colored curves correspond to atoms which are in the interior of the cluster at some point in the simulation, and the grey curves are surface atoms.

metric structure, both of which also possess a double tetrahedral core. Our calculations show that symmetric double-core (i.e. non-crystalline) structures not only have optical gaps similar to those measured experimentally, but form consistently from amorphous silicon nanoclusters in the first few picoseconds of synthesis.

In summary, we find that during the formation process of 1 nm clusters, relaxation of the high strain induced by the curvature and dangling bond states at the surface is in direct competition with the preference of the interior atoms to be tetrahedrally coordinated. Our results show that silicon nanoclusters produced with a high temperature synthesis process consistently form with a non-crystalline, double tetrahedral core. For clusters with 30 silicon atoms, FPMD produced structures with optical gaps in good agreement with both symmetric low-energy structures and experimental measurements. In addition, we find that the stability of small, partially-passivated Si_{29} crystalline fragments strongly depends on the number of hydrogen atoms at the surface, with a crossover from double-core to single-core structures between 12 and 14 hydrogen atoms. This work suggests that the metastable nanostructures most likely to form via a given synthesis process should be classified in terms of both core structure and surface reconstruction.

Acknowledgements The authors thank A. Puzder and F. Reboredo for useful discussions. This work was performed under the auspices of the U.S. Department of Energy by University of California Lawrence Livermore National Laboratory under contract No. W-7405-Eng-48.

References

[1] M. F. Jarrold and J. E. Bower, J. Chem. Phys. **96**, 9180 (1992).
[2] E. C. Honea et al., Nature **366**, 42 (1993).
[3] U. Röthlisberger, W. Andreoni, and M. Parrinello, Phys. Rev. Lett. **72**, 665 (1994).
[4] A. D. Yoffe, Adv. Phys. **50**, 1 (2001).
[5] D. J. Lockwood et al., Solid State Commun. **89**, 587 (1994).
[6] L. T. Canham, Appl. Phys. Lett. **57**, 1046 (1990).
[7] L. N. Dinh et al., Phys. Rev. B **59**, 15513 (1999).
[8] C.-S. Yang et al., J. Am. Chem. Soc. **121**, 5191 (1999).
[9] J. D. Holmes et al., J. Am. Chem. Soc. **123**, 3743 (2001).
[10] T. van Buuren et al., Phys. Rev. Lett. **80**, 3803 (1998).
[11] J. P. Wilcoxon et al., Phys. Rev. B **60**, 2704 (1999).
[12] L. Mitas et al., Appl. Phys. Lett. **78**, 1918 (2001).
[13] G. Allan, C. Delerue, and M. Lannoo, Phys. Rev. Lett. **78**, 3161 (1997).
[14] F. A. Reboredo, A. Franceschetti, and A. Zunger, Appl. Phys. Lett. **99**, 2972 (1999).
[15] GP code, version 1.16.0 User's Manual, F. Gygi, LLNL (2003).
[16] D. M. Ceperley and B. J. Alder, Phys. Rev. Lett. **45**, 566 (1980).
[17] D. R. Hamann, Phys. Rev. B **40**, 2980 (1989).
[18] P. Giannozzi, private communication.
[19] L. Patrone et al., J. Appl. Phys. **87**, 3829 (2000).
[20] G. Belomoin et al., Appl. Phys. Lett. **80**, 841 (2002).
[21] E. W. Draeger et al., Phys. Rev. Let. **90**, 167402 (2003).
[22] W. M. C. Foulkes et al., Rev. Mod. Phys. **73**, 33 (2001).
[23] A. Williamson et al., Phys. Rev. Lett. **89**, 196803 (2002).
[24] CASINO code, version 1.5.4 User's Manual, R. J. Needs et al., University of Cambridge (2002).